Article

Discovery Medicine 2025; 37(200): 1928–1943
https://doi.org/10.24976/Discov.Med.202537200.166

Mitochondrial Metabolic Dysfunction and Immunization in Thyroid Eye Disease: New Insights From Bioinformatics and Machine Learning

Changjun Wang[1], Kai Jin[1], Ji Shao[1], Jingyi Wang[1], Jingxin Zhou[1], Juan Ye[1,*]

[1]Eye Center of the Second Affiliated Hospital, School of Medicine, Zhejiang University, 310009 Hangzhou, Zhejiang, China
*Correspondence: yejuan@zju.edu.cn (Juan Ye)
Submitted: 30 June 2025 Revised: 9 August 2025 Accepted: 22 August 2025 Published: 20 September 2025

Background: Thyroid eye disease (TED) is a common autoimmune inflammatory disease that significantly impairs quality of life. Mitochondrial metabolism is a key driver for the pathogenesis of inflammatory diseases, yet its role in TED remains poorly understood. Our study aimed to investigate the mechanisms by which mitochondrial metabolism contributes to TED and identify potential treatment targets using a multi-methodological approach.

Methods: We performed a series of bioinformatics analyses, including the identification of differentially expressed genes (DEGs), Kyoto Encyclopaedia of Genes and Genomes (KEGG) enrichment analysis, immune infiltration assessments, genome-wide association studies (GWAS), and machine learning.

Results: By integrating the datasets GSE58331, GSE105149, and GSE185952, we ultimately screened 14 mitochondria-related (DEGs) from TED samples and applied machine learning to select diagnostic markers. 3 disease-associated diagnostic biomarkers (*Ifi27*, *Cyba*, and *Cmpk2*) were identified. Immune cell infiltration analysis revealed 4 immune cell types significantly associated with TED: follicular helper T (Tfh) cells, monocytes, M1 macrophages, and neutrophils. Multiple specific correlations were observed between these immune cells and the diagnostic biomarkers.

Conclusion: We identified a unique mitochondrial-related genetic signature essential for TED progression, which provides valuable insights into immune infiltration. These findings may advance molecular research on TED and offer novel strategies and therapeutic approaches for this condition.

Keywords: thyroid eye disease; mitochondria-related DEGs; Gene Set Enrichment Analysis; immune infiltration; Kyoto Encyclopaedia of Genes and Genomes

Introduction

Thyroid eye disease (TED), often referred to as Graves' ophthalmopathy, Graves' orbitopathy, or thyroid-associated ophthalmopathy (TAO), is typically associated with Graves' hyperthyroidism (GH)—a post-globular autoimmune disorder [1]. TED is characterised by a systemic autoimmune attack targeting the orbits and other tissues, including the thyroid, skin, and anterior tibialis soft tissues [2]. Common clinical manifestations include eyelid retraction, impaired ocular motility, diplopia, and exophthalmos. In severe cases, dysthyroid optic neuropathy (DON) can result in irreversible blindness [3–5]. The annual incidence of TED is approximately 16 cases per 100,000 women and 3 cases per 100,000 men [6]. TAO impairs patients' visual function and craniofacial appearance, thereby reducing their quality of life. Therefore, screening and early diagnosis of TAO—which enable timely and effective management of the condition—can alleviate the physical and psychological burdens on patients [7]. Due to the wide spectrum of clinical manifestations, available treatment options range from supportive therapy to surgical intervention. Although glucocorticoids [7] and targeted agents (tolizumab [8] and teprotumumab [9]) can provide partial benefits to patients, a satisfactory response remains rare [10]. Additionally, treatment options are limited for patients who are unresponsive to or intolerant of immunosuppressive therapies. Thus, gaining insight into the underlying molecular mechanisms of TED is vital to creating novel therapeutic strategies that can effectively treat the disease, prevent its recurrence, and improve patient outcomes.

Mitochondria are essential organelles that maintain cellular energy metabolism and serve as signalling hubs for preserving cellular biological functions [11]. Growing evidence has demonstrated a strong correlation between mitochondrial dysfunction and the onset and progression of various ocular diseases. In addition to generating Adenosine triphosphate (ATP), mitochondria are a major source of reactive oxygen species (ROS) via oxidative phosphorylation (OXPHOS). Impaired mitophagy has been reported to enhance oxidative damage and induce mitochondrial energy defects, thereby promoting the progression of disease,

such as tumorigenesis [12], neuroinflammation [12] and intestinal diseases [13]. Moreover, mitochondrial impairment and oxidative stress in the retinal pigment epithelium are thought to play a significant role in the development of age-related macular degeneration [14]. Molecular danger signals released ROS-producing damaged mitochondria trigger a robust inflammatory response via pattern recognition receptors (PRRs) [15]. Abnormal mitochondrial metabolism in immune cells has been documented in autoimmune diseases, including rheumatoid arthritis [16] and systemic lupus erythematosus [17]. Accumulating evidence has revealed a potential link between immunity and mitochondrial metabolism, suggesting that metabolic status can influence inflammatory processes by modulating the immune microenvironment. Abnormal mitochondrial metabolism is a key mechanism driving inflammation in chronic disease processes; however, its role in TED and its interaction with immune cells remain unreported and require further investigation.

Bioinformatics facilitates the identification of differentially expressed molecules between control and disease groups by leveraging microarray data that exhibit variations across multiple levels. This approach is widely recognized as a valuable research tool for investigating the underlying molecular mechanisms of diseases. In the present study, we identified a significant association involving mitochondria-related genes using relevant microarray data from the Gene Expression Omnibus (GEO) dataset in TED. Furthermore, we employed machine learning to identify mitochondria-related diagnostic genes and validate their accuracy for TED. Additionally, an immune infiltration analysis was conducted to explore potential correlations between differentially expressed genes (DEGs) and immune cells. The objective of our research is to enhance the understanding of how mitochondria-related genes contribute to TED and provided novel strategies for the diagnosis and treatment of this condition.

Methods

Acquisition and Processing of RNA Sequencing (RNA-seq) Data

Here, we followed the methods described by Chenyan Zhang *et al.* [18]. Two sets of raw RNA-seq data for TED patients were extracted from the GEO databases: GSE58331 (https://www.ncbi.nlm.nih.gov/geo/query/acc.cgi?acc=GSE58331) and GSE105149 (https://www.ncbi.nlm.nih.gov/geo/query/acc.cgi?acc=GSE105149). The GSE58331 expression profile, which includes 8 TED samples and 7 control samples, was analyzed with GPL570HG-U133_Plus_2. Similarly, the GSE105149 dataset, comprising 4 TED samples and 7 control samples, was analyzed using the GPL570HG-U133_Plus_2. Another validation GSE185952 dataset (https://www.ncbi.nlm.nih.gov/geo/query/acc.cgi?acc=GSE185952), including 3 TED samples and 3 control samples) was processed using the platform of GPL30862 Agilent- 086360 Shbio Human (4 × 180 K) array. The gene expression matrices were constructed by processing the raw RNA-seq data, and the entire analytical procedure was performed using R software (version 4.4.1, maintained by the R Foundation for Statistical Computing, Vienna, Austria).

GO and KEGG Analysis

The "clusterprofile" package (v4.12.6, hosted on Bioconductor (https://bioconductor.org/), Hong Kong, China) [19,20] was employed to perform Gene Ontology (GO) enrichment analysis on the DEGs, with a significance threshold where the p-value was set to <0.05. Besides, pathway enrichment, including Kyoto Encyclopaedia of Genes and Genomes (KEGG) Pathways and WikiPathways, was analyzed for the DEGs using Enrichr (https://maayanlab.cloud/Enrichr/).

Acquisition for Mitochondria-Related DEGs (MitoDEGs)

A total of 1136 mitochondria-related genes were retrieved from MitoCarta3.0, a mitochondrial protein database (http://www.broadinstitute.org/mitocarta). From the matrices of the GSE58331 dataset and GSE105149 datasets, DEGs between TED and control samples were screened using the "limma" package (v3.60.5, hosted on Bioconductor, Melbourne, Victoria, Australia) [21]. Genes with $|\log2FC| > 0.585$ and a p-value < 0.05 were considered to be significantly differentially expressed (DEGs) [22]. The screened DEGs were visualized via volcano plots generated with the R package "ggplot2" (v3.5.1) [23], and heatmaps created using the R package "ComplexHeatmap" (v2.20.0, hosted on Bioconductor (https://bioconductor.org/), Hong Kong, China) [24]. MitoDEGs were identified as the intersection of mitochondria-related genes and DEGs using Jvenn [25].

Construction of PPI Networks and Hub Gene Discovery

The protein-protein interaction (PPI) networks of MitoDGEs were retrieved from the STRING database (https://string-db.org/). For network construction, gene interactions with a combined score of ≥ 0.4 were selected, and these PPI networks were visualized using Cytoscape (v3.8.2, Cytoscape Consortium, Seattle, WA, USA). Subsequently, hub MitoDEGs were identified using the Cytoscape plug-in CytoHubba based on various algorithms.

Acquisition of Hub MitoDEGs Is Key to TED

To identify genes critical to TED, we further analyzed the association between hub mitochondrial differentially expressed genes (hub MitoDEGs) and the risk of TED development using the Comparative Toxicogenomics Database (CTD; http://ctdbase.org/). The CTD database is

an online resource that compiles information on interactions between drug-gene products, functional phenotypes, and their relationships to diseases, and it was used here to investigate disease-associated genes and medical drug-gene interactions [26].

Hub MitoDEGs-Regulatory Network Construction

Transcription factors (TFs) were retrieved from the JASPAR database (https://jaspar.elixir.no/), an improved open-access repository of transcription factor binding profile. Subsequently, we analyzed the JASPAR database utilizing the NetworkAnalyst platform (https://www.networkanalyst.ca/) to identify topologically viable TFs commonly associated with our hub MitoDEGs. NetworkAnalyst is an online platform specifically designed to facilitate meta-analysis of gene expression data, thereby enabling a comprehensive examination of biological mechanisms and their resulting effects. Concurrently, the 'NetworkAnalyst' tool was used to identify miRNAs associated with these hub MitoDEGs from MiRTarBase, the primary online repository for miRNA and target gene relationships [18,27].

Immune Infiltration Analysis

The immune cell composition in both the TED group and the control group was analyzed using the "CIBERSORT" package (v1.0, Stanford University, Stanford, CA, USA), a tool that deconvolves the expression matrix of immune cell subtypes by applying the principle of linear support vector regression. It is the most frequently cited analytical tool for estimating immune cell infiltration.

GSEA Analysis

Gene Set Enrichment Analysis (GSEA) enables in-depth exploration of biological processes perturbed under specific phenotypic or disease conditions. This is achieved by ranking genes according to their differential expression patterns and leveraging a collection of predefined gene sets [28]. GSEA was conducted to investigate the potential molecular mechanisms and signaling pathways of hub MitoDEGs in TED patients using the "clusterProfiler" package [28]. The "c2.cp.v7.2.symbols.gmt", file was selected as the reference gene set for analysis. The enriched pathways were ranked by normalized enrichment scores, and those with a p-value < 0.05 were selected for further analysis. A total of 1000 permutations were performed, with the permutation targeting the phenotype. This indicates that phenotype labels were randomly rearranged during the analysis. The results were visualized using the "ggplot2" package.

Machine Learning Analysis

For machine learning analysis, least absolute shrinkage and selection operator (LASSO) regression was performed on these hub MitoDEGs using "glmnet" package (v4.1.8, CRAN, Stanford, CA, USA) [29]. In addition to these methods, the Support Vector Machine Recursive Feature Elimination (SVM-RFE) algorithm and the Random Forest (RF) algorithm were employed to screen for potential candidate genes. LASSO regression was employed to select feature variables and construct the optimal classification model by identifying for the λ value ($\lambda = 0.02299332$) that minimizes classification error. The SVM-RFE algorithm, a machine learning technique based on support vector machine principles, works by searching for the optimal SVM model using the complete feature set within the dataset, and the "e1071" package (v1.7.16, CRAN, Vienna, Austria) was employed for its implementation. The RF algorithm, a machine learning approach built on decision tree algorithms, is implemented using the "randomForest" package (v4.7.1.2, CRAN, Kenilworth, NJ, USA) and is widely used to address both regression and classification problems. With notable robust performance even with small sample sizes [30]. In this study, the outputs of the three machine learning algorithms were intersected to identify genes with potential diagnostic value for TED. The intersection results were subsequently visualized and subjected to further analysis.

Genome-Wide Association Study (GWAS Analysis)

GWAS analysis of the genes was performed using the Gene Atlas database (http://geneatlas.roslin.ed.ac.uk/). Derived from the UK Biobank cohort, this database serves as a comprehensive archive containing associations among multiple traits and millions of variants, including 778 phenotypes and 30 million loci. This large-scale database enables the identification of genetic variations associated with specific traits or diseases, thereby facilitating an in-depth understanding of the underlying biological mechanisms.

Statistical Analyses

Differences between two groups were evaluated using an unpaired Student's t-test, while differences among multiple groups were analyzed using one-way or two-way ANOVA, followed by a Tukey *post-hoc* test. For correlation analysis, the Spearman rank-order correlation test was employed. Statistical significance was set at a p-value < 0.05.

Results

Identification of DEGs in TED

The study flowchart is depicted in Fig. 1. Two TED-related GEO datasets, GSE58331 and GSE105149, were downloaded for analysis. After excluding genes without matching gene symbols, differential analysis identified 7085 DEGs in the GSE105149 dataset, including 2484 downregulated genes and 4601 upregulated genes; 3952 DEGs were screened in the GSE58331, comprising 2541 downregulated genes and 1411 upregulated genes. These DEGs were displayed as volcano plots and heatmaps (Fig. 2A–D and **Supplementary Table 1**). Subsequently,

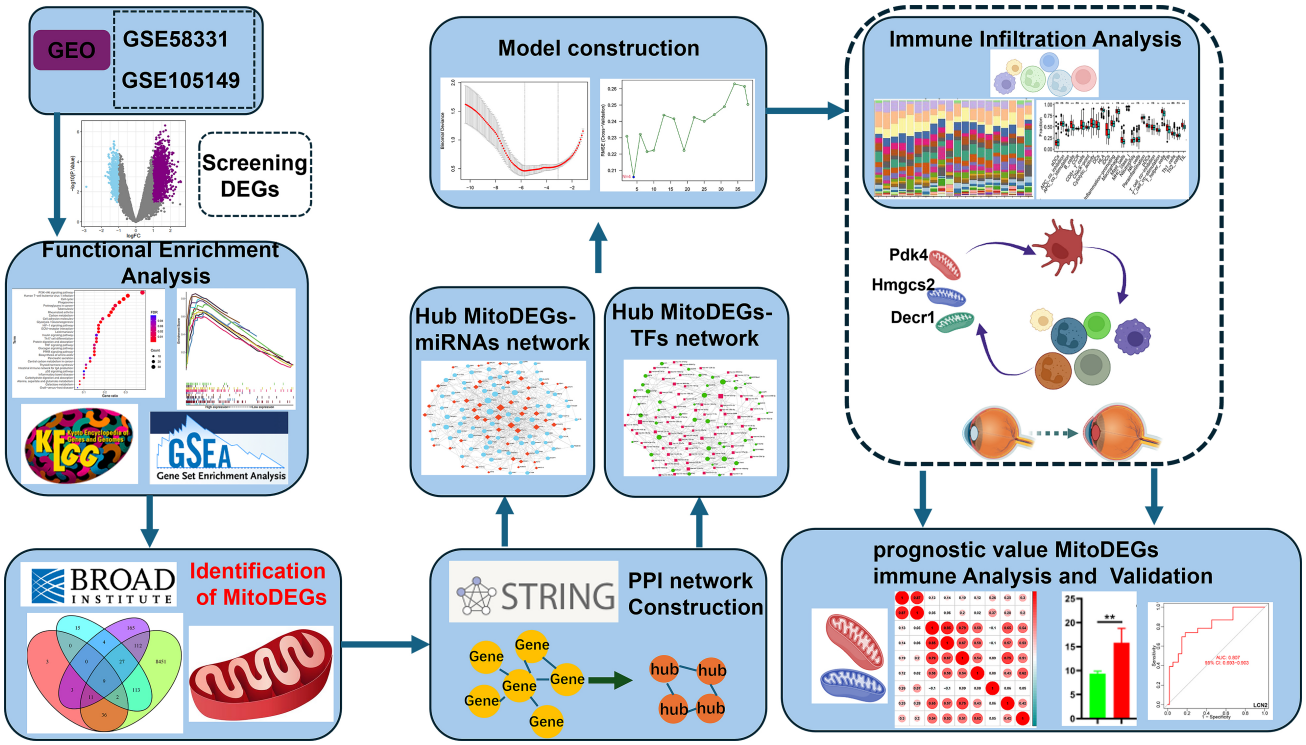

Fig. 1. Workflow diagram of the study. GEO, Gene Expression Omnibus; DEGs, differentially expressed genes; KEGG, Kyoto Encyclopaedia of Genes and Genomes; GSEA, Gene Set Enrichment Analysis; PPI, protein-protein interaction. $^{**}p < 0.01$. Created by Photoshop 2023 (Adobe Inc., San Jose, CA, USA).

we further analyzed potential signaling pathways associated with DEGs using GSEA. As shown in **Supplementary Fig. 1** and **Supplementary Table 2**, most DEGs across the two datasets were associated with pathways such as adherens junction, the spliceosome, the proteasome, and the tight junction.

Enrichment Analysis of DEGs in TED

Functional and pathway enrichment analyses of the DEGs were conducted using GO and KEGG analyses. The results showed that DEGs from the two datasets were primarily enriched in the GO-biological process (BP), including negative regulation of programmed cell death, apoptotic process, and negative regulation of apoptotic process. For GO-cell component (CC), these DEGs were mainly enriched in the focal adhesion, nucleolus, and nucleus and cell-substrate junction. Meanwhile, in terms of GO-molecular function (MF), the DEGs were primarily enriched in cadherin binding and RNA binding (Fig. 3A,D and **Supplementary Tables 3,4**). Additionally, KEGG enrichment analysis results revealed that DEGs from the two datasets were significantly enriched in pathways, such as protein processing in the endoplasmic reticulum, autophagy, shigellosis, pathogenic escherichia reticulum, the peroxisome proliferator-activated receptors (PPAR) signaling pathway, the mechanistic target of rapamycin (mTOR) signaling, Th17 cell differentiation and the Hippo signaling pathway (Fig. 3B,C,E,F and **Supplementary Tables 5,6**). Furthermore, the results of the WikiPathways (WP) enrichment analysis indicated that these DEGs were significantly enriched in vascular endothelial growth factor A (VEGFA)/vascular endothelial growth factor receptor 2 (VEGFR2) signaling pathway, mRNA processing, G protein signaling pathway, epidermal growth factor (EGF)/epidermal growth factor receptor (EGFR) signaling pathway, IL24 signaling pathway, Interleukin 1 (IL1) structural pathway, and TGF-β signaling pathway (**Supplementary Fig. 2A–D** and **Supplementary Tables 4,6**).

Identification MitoDEGs in TED

To further identify mitochondrial metabolic-related genes in TED, mitochondrial-related genes were retrieved from the MitoCarta3.0 dataset. These genes were overlapped with the DEGs from the two TED datasets, and was identified as mitochondrial-related DEGs (MitoDEGs). A total of 160 MitoDEGs were identified, including 68 downregulated genes and 92 upregulated genes in TED samples compared to normal samples (Fig. 4A,B). A PPI network was constructed using the STING databases to further explore the interactions between the above MitoDEGs. As shown in Fig. 4C, 989 nodes were visualized using the Cytoscape program. Additionally, hub genes among these MitoDEGs were identified using the Cytoscape plug-in "cyto-

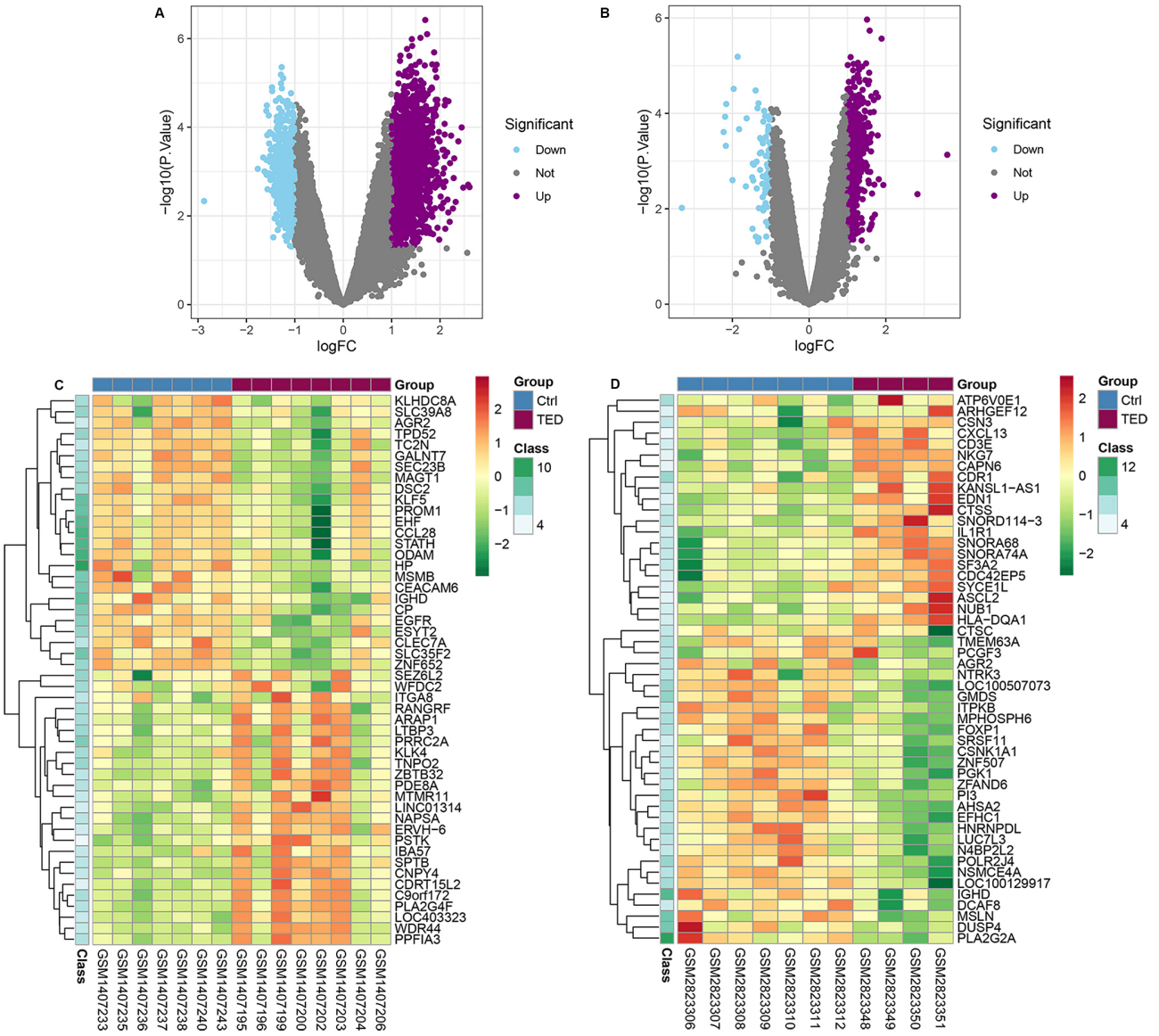

Fig. 2. Identification of DEGs between normal and thyroid eye disease (TED) groups. (A,B) DEGs were identified in the GSE58331 dataset (A) and GSE105149 dataset (B) displayed in the volcano plot. Cut-offs were set at $|\log2FC| > 0.585$ with $p < 0.05$ indicating significance. Red dots represent upregulated DEGs, while green dots represent downregulated DEGs. (C,D) The heatmap of DEGs between normal and TED groups. Green: low expression level; Red: high expression level.

Hubba" based on the degree of connectivity scores via four algorithms: Degree, Maximal Clique Centrality (MCC), Density of Maximum Neighborhood Component (DMNC) and Maximum Neighborhood Component (MNC). After integrating the top 50 hub genes from each of the four algorithms, 30 common hub genes were identified across all four algorithms (Fig. 4D,E). These common hub genes from both datasets were then visualized separately using heatmaps (Fig. 4F,G).

Relationship Between TED and Hub MitoDEGs

To further identify genes significantly associated with TED, the CTD dataset was utilized to predict the relationship between TED and hub MitoDEGs. Consequently, 14 genes exhibited the strongest association with TED among these 30 common hub MitoDEGs (Fig. 5A,B).

Prediction of TFs and miRNAs Regulatory Network Analysis of TED-Related Hub MitoDEGs

Subsequently, we employed a network-based approach to investigate regulatory TFs and post-transcriptional miRNAs, with the aim of characterizing the regulatory molecules associated with TED-related hub MitoDEGs. The resulting TFs-miRNAs-Hub MitoDEGs regulatory network was visualized using Cytoscape. Fig. 5C,D provides a comprehensive overview of the 43 TFs and 17 miRNAs that exerted regulatory control over

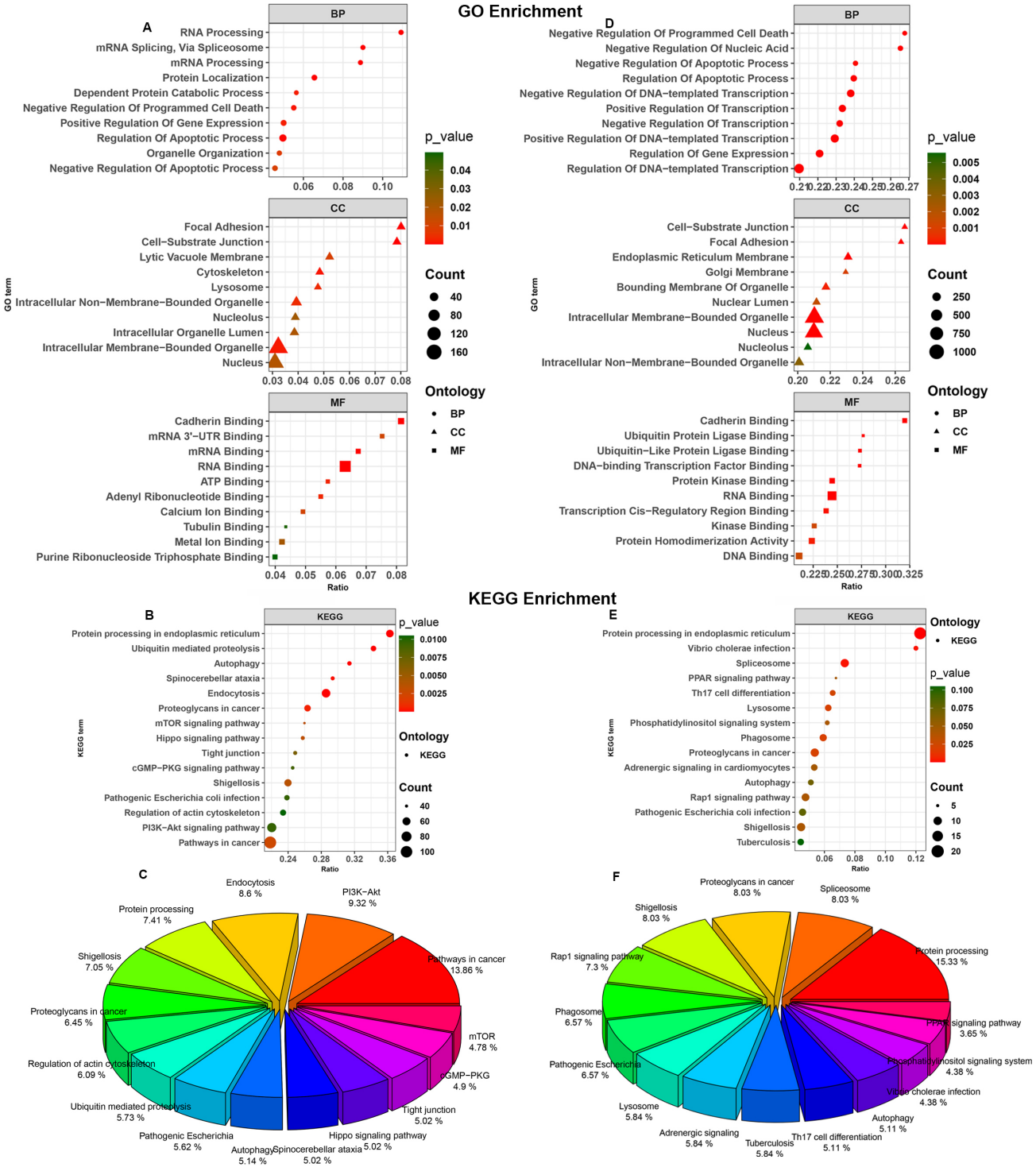

Fig. 3. Enrichment analysis of functions and pathways for DEGs from GSE58331 and GSE105149. (A,D) The enriched Gene Ontology (GO) terms of DEGs in GSE58331 and GSE105149. (B,C,E,F) KEGG pathway enrichment results of DEGs in GSE58331 and GSE105149.

multiple TED-related hub MitoDEGs. These findings suggest that these TFs or miRNAs may have potential regulatory effects on the expression levels of hub genes. However, further research is required to validate these observations.

Immune Infiltration in TED

TED is an inflammatory disorder characterized by orbital tissue involvement. To better elucidate the immunomodulation processes in TED, immune cell infiltration patterns were assessed utilizing the CIBERSORT al-

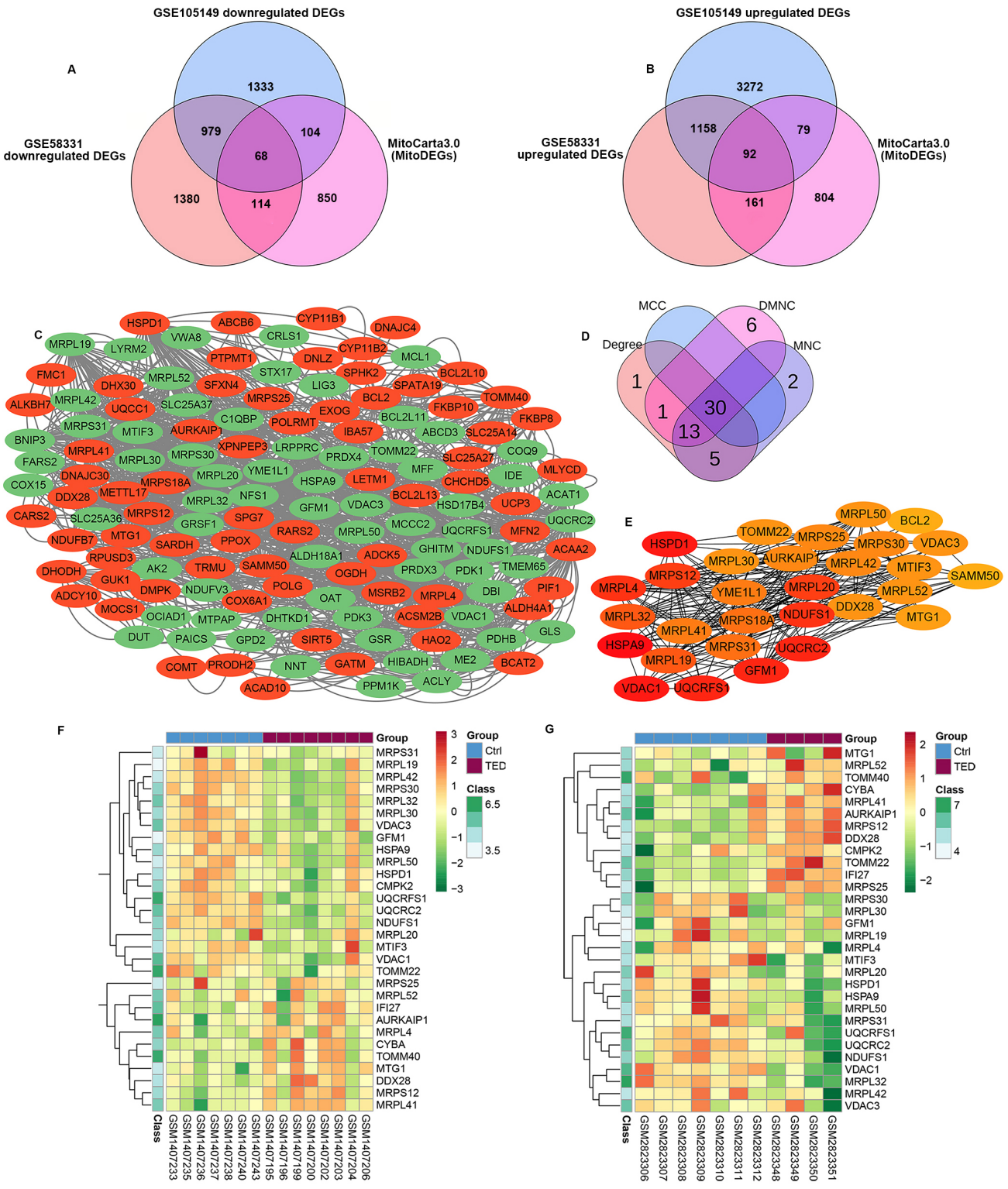

Fig. 4. Construction of the PPI network and identification of hub MitoDEGs. (A,B) Venn diagrams illustrated the number of overlapping downregulated and upregulated DEGs among the GSE58331 dataset, GSE105149 dataset, and MitoCarta3.0 database. (C) PPI networks construction of MitoDEGs. (D) Venn diagram of the hub MitoDEGs extracted by the three algorithms based on the Cytohubba. (E) The network of the common 30 hub MitoDEGs were displayed in Cytoscape. (F,G) The heatmap of 30 hub MitoDEGs both in GSE58331 and GSE105149.

gorithm. The bar plot (Fig. 6B) displays the proportion of each of the 22 immune cell types in individual samples from both the TED and control groups. Compared to the control group, the TED group exhibited higher levels of fol-

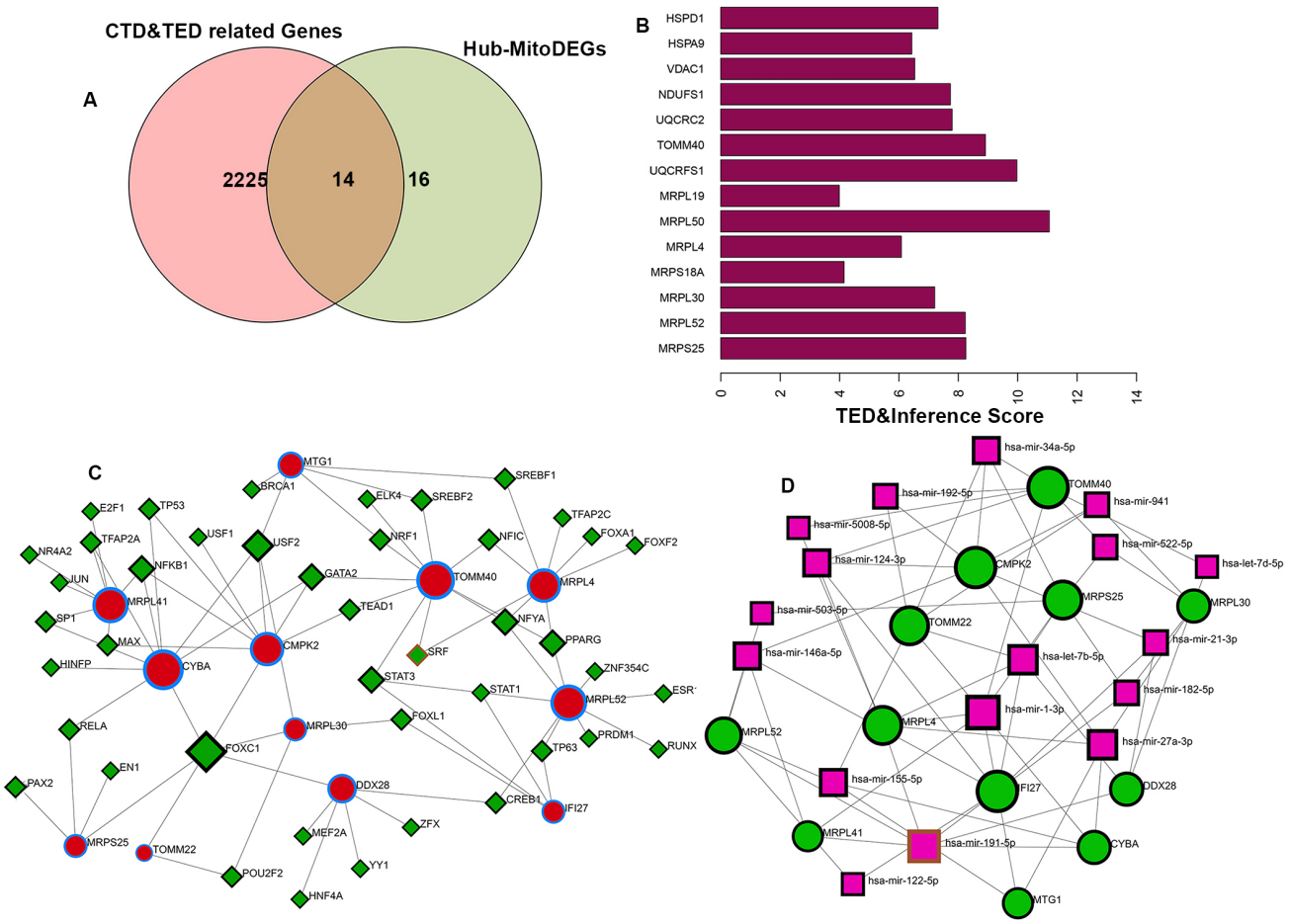

Fig. 5. Associations between hub MitoDEGs and TED. (A,B) Hub MitoDEGs related to TED based on the Comparative Toxicogenomics Database (CTD) database. (C) The regulatory network of TF–hub MitoDEGs: The red dots indicate MitoDEGs and green squares indicate TFs. (D) miRNA–hub MitoDEGs regulatory network: The green dots indicate MitoDEGs and pink squares indicate miRNA.

licular helper T cells, monocytes, M1 macrophages, and neutrophils. In contrast, the proportion of plasma cells was lower in the TED group (Fig. 6A–C). Further analysis of immune cell infiltration in TED revealed multiple correlations between immune cell types. Correlation analysis of the 22 immune cell types revealed that monocytes were positively associated with dendritic cells (r = 0.64), neutrophils were positively related to activated mast cells (r = 0.61), M1 macrophages were positively correlated with regulatory T cells (r = 0.61), memory B cells were positively related to $CD8^+$ T cells (r = 0.56), and M1 macrophages were negatively associated with plasma cells (r = –0.56) (Fig. 6D). These findings indicated that various immune cells exhibit differential infiltration in TED patients, which may serve as a potential target for modulating TED treatment.

The Screen of Potential Candidate Genes for TED via Machine Learning

Subsequently, we employed the LASSO regression, SVM-RFE, and RF machine learning algorithms to identify candidate genes for nomogram development and diagnostic value assessment based on GSE58331 and GSE105149 dataset. As shown in Fig. 7A–C, the LASSO regression algorithm and SVM-RFE identified 4 and 8 potential candidate biomarkers, respectively. Furthermore, the RF algorithm prioritizes genes based on their assessed significance (Fig. 7D,E). The intersection of the 4 most significant genes from the RF analysis, the 4 prospective candidate genes obtained from the LASSO regression, and 8 potential prognostic genes in SVM-RFE was visualized via a Venn diagram. A total of 3 genes (*Ifi27*, *Cyba* and *Cmpk2*) were identified as potential diagnostic markers for final validation (Fig. 7F). We further assessed the predictive value of the 3 potential markers using datasets GSE58331 and GSE105149. In both datasets, *Ifi27*, *Cyba* and *Cmpk2* were significantly upregulated in the TED samples compared to the control samples (Fig. 7G and **Supplementary Fig. 3A**). Additionally, receiver operating characteristic (ROC) analysis confirmed that *Ifi27*, *Cyba* and *Cmpk2* could accurately predict TED, with AUC of 0.887, 0.810 and 0.815 in GSE58331 (Fig. 7H), and 0.768, 0.821 and 0.750 in GSE105149 (**Supplementary Fig. 3B**). We then analyzed the expression levels and ROC analysis of these three genes in another dataset (GSE58331, including 27 orbital tissue

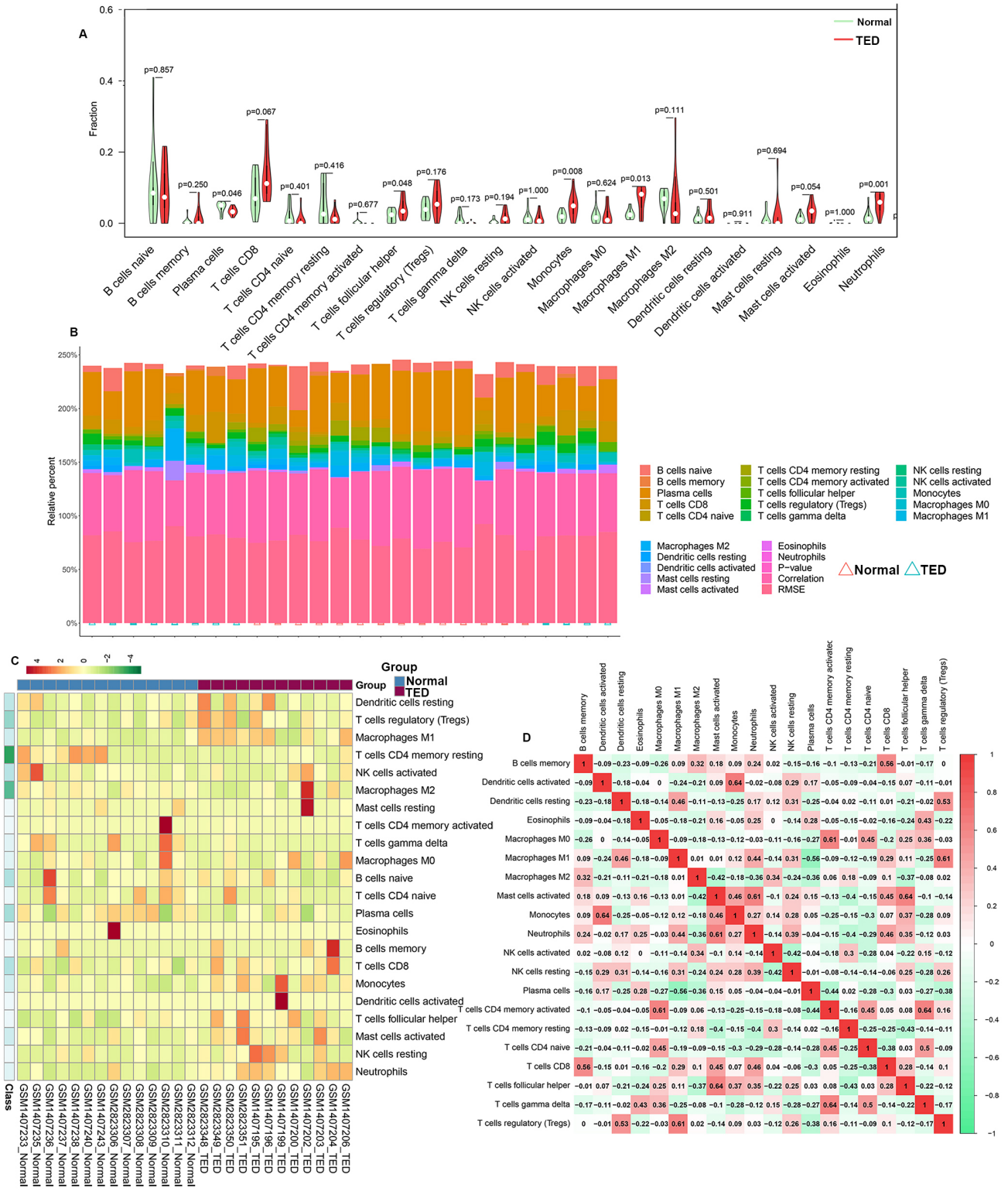

Fig. 6. Expression of immune cells. (A) Expression levels of immune cells in the normal group versus the TED group. (B) Stacked bar graphic illustrating the distribution of immune cells. (C) Heatmap depicting the distributions of the 22 immunological cell types. (D) Analytical of the correlation among several immune cell types. not significant, $p > 0.05$; significant, $p < 0.05$ (unpaired two-tailed Student's t test; mean ± SD).

samples and 21 control tissue samples) and analyzed the expression levels of these genes in GSE185952 dataset (3 orbital tissue samples and 3control tissue samples). The results indicated that the mRNA levels of all three genes were upregulated in the orbital tissue from TED patients compared to healthy controls (**Supplementary Fig. 3C,E**).

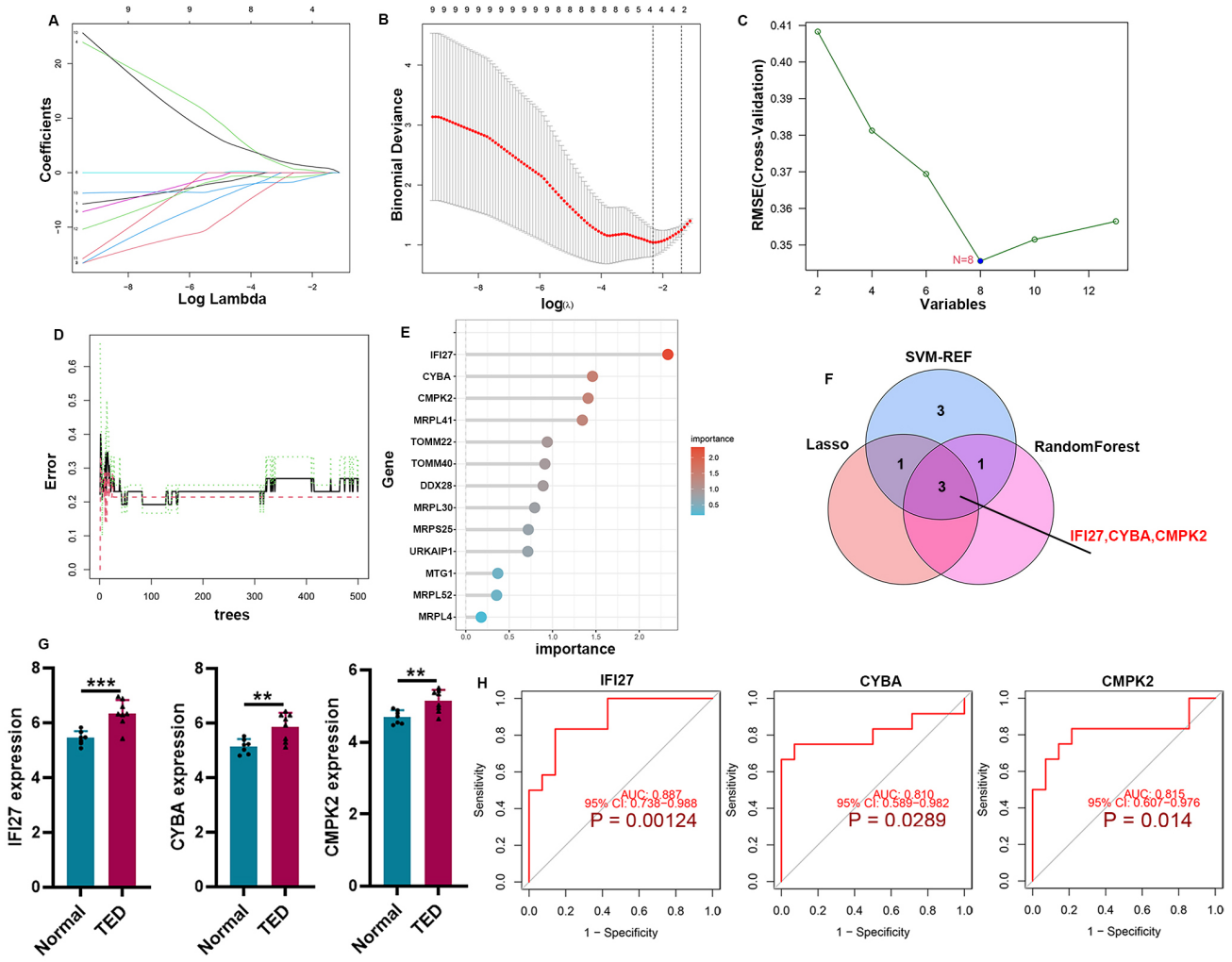

Fig. 7. Identification and validation of diagnostic biomarkers for TED in GSE58331 and GSE105149. (A) Cross-validation for least absolute shrinkage and selection operator (LASSO) regression to fine-tune parameter selection. (B) The LASSO logistic regression analysis of hub MitoDEGs. (C) Support Vector Machine Recursive Feature Elimination (SVM-RFE) algorithm analysis of hub MitoDEGs. (D) Analyzing DEGs with a random survival forest. (E) 4 genes were identified as final markers with varied relative relevance >1. (F) Venn showing intersection of lasso, Random Forest (RF) and SVM-RFE core genes. (G) The expression of diagnostic biomarkers based on the GSE58331 dataset. (H) The receiver operating characteristic (ROC) curve of diagnostic biomarkers based on the GSE58331 dataset. $^{**}p < 0.01$, and $^{***}p < 0.001$ (unpaired two-tailed Student's *t* test; mean ± SD).

In addition, these genes showed a high diagnosis value for TED patients, with a ROC of 0.869, 0.739 and 0.721 (**Supplementary Fig. 3D**).

Correlation Analysis of Immune Cells and Hub MitoDEGs

Next, the potential association between hub MitoDEGs and immune cells were analyzed using the Spearman's rank correlation method. Fig. 8A–C illustrates the positive and negative associations between these three potential genes (*Ifi27*, *Cyba* and *Cmpk2*) and immune cells. Among three potential genes, *Ifi27* was positively associated with neutrophils, monocytes and M1 macrophages but negatively correlated with naïve B cells, naïve $CD4^{+}$T cells, and gamma delta T cells ($\gamma\delta$T cells). *Cyba* showed positively associated with neutrophils, monocytes, M1 macrophages and regulatory T cells. *Cmpk2* was positively associated with neutrophils, monocytes, M1 macrophages and activated mast cells while negatively associated with memory B cells.

GSEA Enrichment Analysis of the Hub MitoDEGs

Based on the characterization of the diagnostic genes, *Ifi27*, *Cyba* and *Cmpk2* were identified as the genes most likely to be associated with TED. We then explored the impact of these three genes on signaling pathways involved in TED pathogenesis by analyzing the specific signaling pathways associated with these potential genes. GSEA results showed that the high expression of *Ifi27* and *Cyba* was mainly enriched in pathways such as Type I diabetes mel-

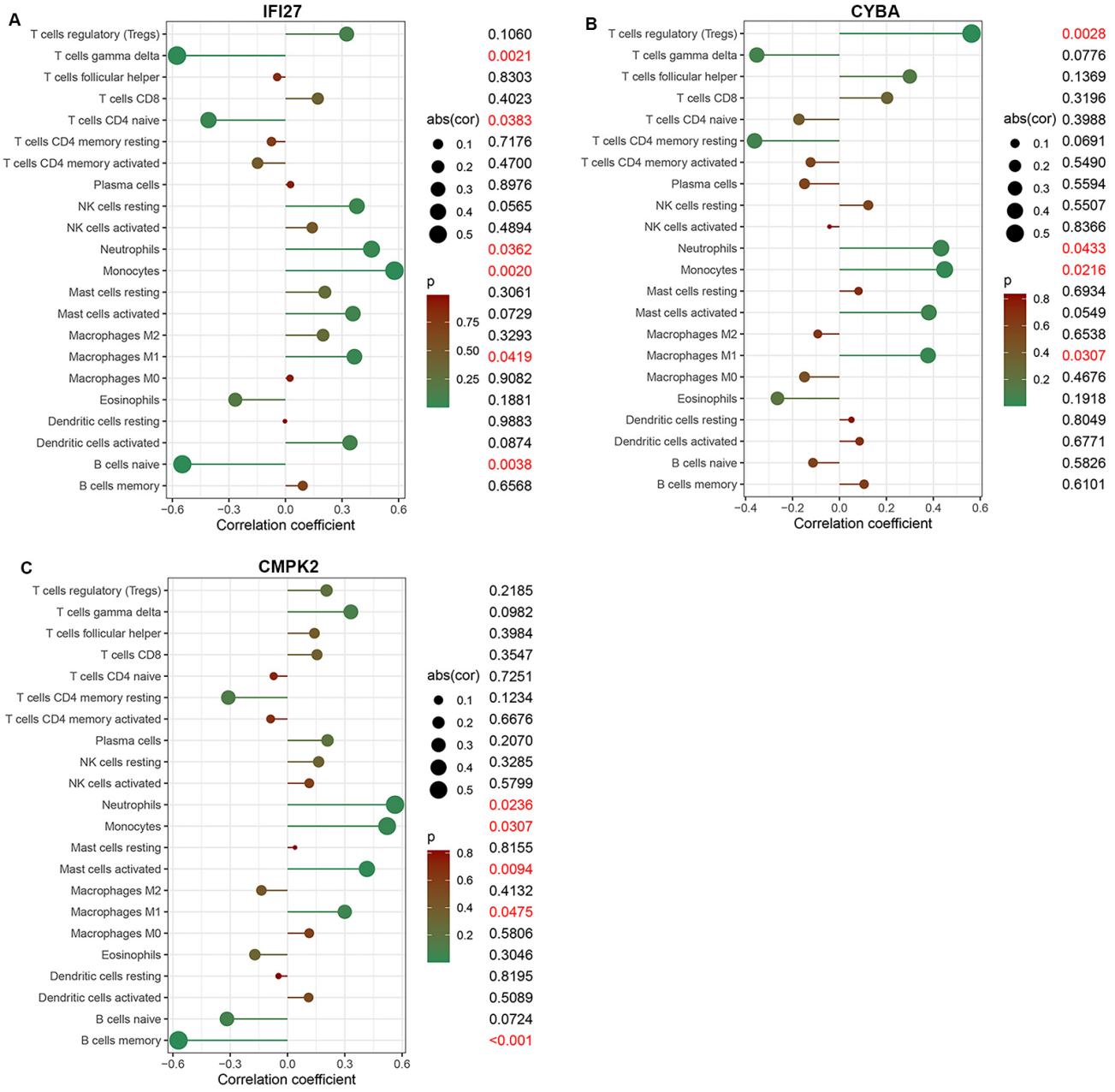

Fig. 8. Examination of the relationship between immune cells and diagnostic biomarkers. (A–C) Correlation analysis between the immune cells and *Ifi27*, *Cyba* or *Cmpk2*. not significant, $p > 0.05$; significant, $p < 0.05$ (the red data) (unpaired two-tailed Student's *t* test; mean ± SD).

litus, Systemic lupus erythematosus, and Asthma. In contrast, the high expression of *Cmpk2* was primarily enriched in signaling pathways, including Vibrio cholerae infection, Protein export, and Proteasome (**Supplementary Fig. 4**).

GWAS Analysis of Hub Genes

To further investigate the mechanisms by which these three genes contribute to TED, we identified the pathogenic regions of these three candidate genes in TED through analysis of GWAS data (Fig. 9A,B). Additionally, the pathogenic regions of single nucleotide polymorphisms (SNPs) corresponding to the three candidate genes—*Ifi27*, *Cyba* and *Cmpk2* are presented. The results revealed that *Ifi27* is located within the pathogenic region of chromosome 14, *Cyba* resides in the pathogenic region of chromosome 16, and *Cmpk2* is situated in the pathogenic region of chromosome 2 (Fig. 9C–E).

Discussion

Thyroid eye disease (TED) is one of the most common autoimmune inflammatory diseases, exerting a profound impact on both the physical and mental well-being

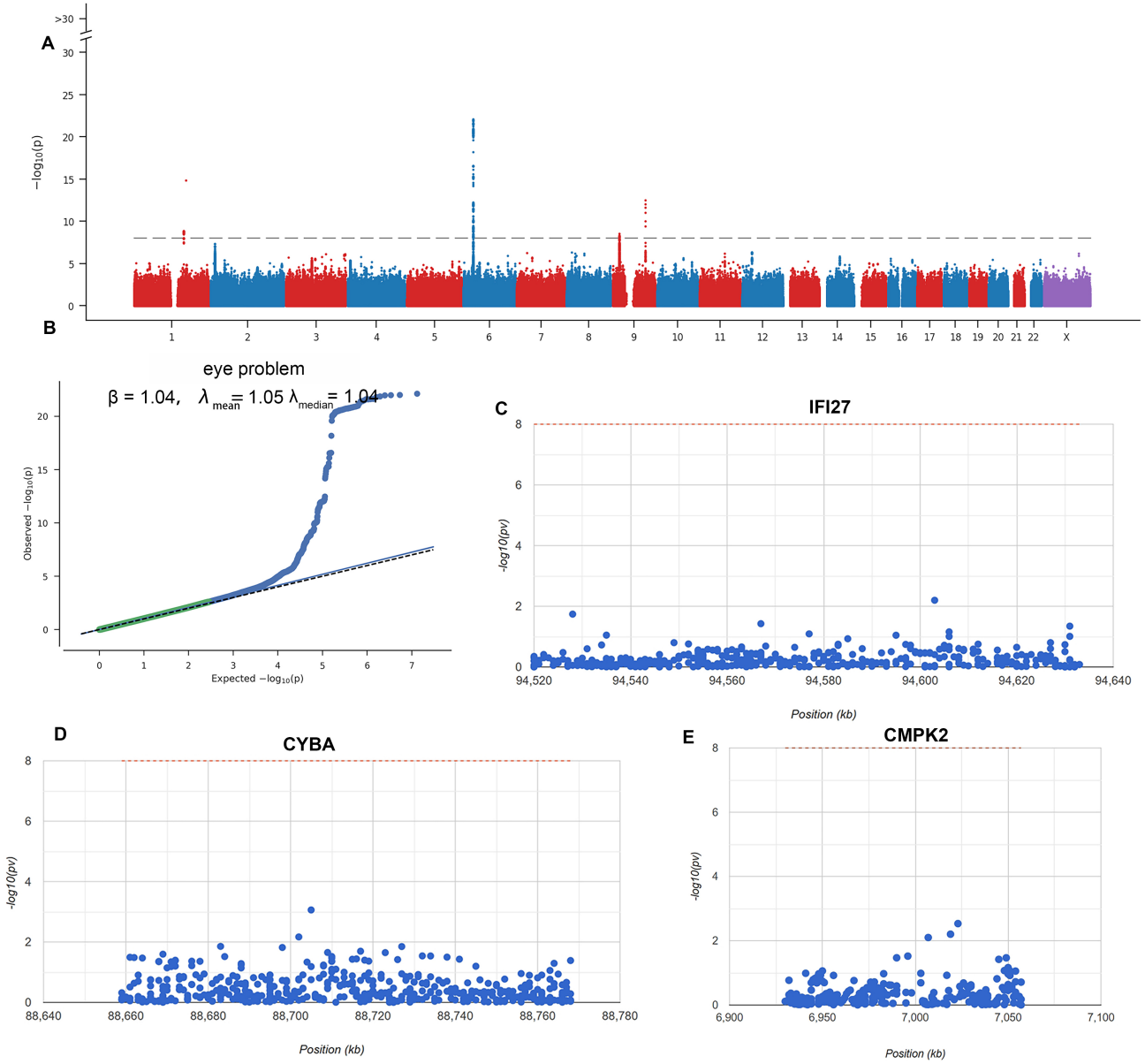

Fig. 9. Genome-wide association studies (GWAS) analysis of *Ifi27*, *Cyba* or *Cmpk2*. (A) Manhattan plot of the GWAS. (B) Q-Q plot of the GWAS. (C) Chromosomal localization of *Ifi27* in the pathogenic region of chromosome 14. (D) Chromosomal location of *Cyba* inside the pathogenic region of chromosome 16. (E) *Cmpk2* was situated in the pathogenic locus of chromosome 2.

of affected patients [31]. Unfortunately, current therapeutic approaches for TED cannot satisfactorily alleviate the inflammatory response during the acute phase of the disease or correct its long-term sequelae [32]. Furthermore, its precise molecular mechanisms have not been fully elucidated. In this context, it is essential to improve our understanding of the etiology of TED and identify potential therapeutic targets. Here, MitoDEGs were obtained from the TED-related microarray dataset and the MitoCarta3.0 database using multiple bioinformatics approaches. Subsequently, we conducted functional and pathway enrichment analyses of these MitoDEGs utilizing GO, KEGG and GSEA. We performed a correlation analysis between TF/miRNA and MitoDEGs and identified disease-related diagnostic genes through multiple deep machine learning analyses and correlation analyses with immune cells in TED. This study aimed to investigate mitochondrial metabolism and its regulatory role in TED pathogenesis, as well as to explore related targets. The results of this study may enhance our understanding of mitochondrial metabolic pathways in TED, along with immunity and their interactions in the disease.

Currently, there remains a gap in the bioinformatics research on mitochondria-related genes in TED. For the first time, we retrieved mitochondria-related genes from the MitoCarta3.0 database and identified 160 MitoDEGs associated with TED. Three potential targets—*Ifi27*, *Cyba* and *Cmpk2*, were identified through the integration of a multimodal analysis model, along with the CTD database, Lasso

regression, SVM-RFE and RF algorithms. Validation using external datasets confirmed the high expression of these three genes in TED patients and diagnostic value.

Mitochondrial metabolism dysfunction is one of the key pathogenetic mechanisms in chronic inflammation-related disease [33]. Elevated expression of Interferon alpha (IFN-α) inducible protein 27 (IFI27) has been shown to be associated with immune response and mitochondrial dysfunction [34]. Research has shown that IFI27 contributes to tumorigenesis by regulating IFN-induced apoptosis, cell proliferation, and immune responses [35]. Additionally, IFI27 is significantly upregulated in salivary gland samples from Primary Sjogren's syndromes (pSS), where it induces IFN-α secretion to drive disease progression [34]. Consistent with these findings, increased IFI27 transcript levels have been observed in TED patients. Cytidine monophosphate kinase 2 (CMPK2) is a mitochondrial nucleotide monophosphate kinase that regulates mitochondrial DNA synthesis. Its deficiency can lead to mitochondrial DNA depletion syndrome [36], reducing ATP production and causing structural disorganisation of mitochondrial cristae [37]. Experimental evidence has demonstrated that upregulated CMPK2 enhances IFN-α-induced ROS production and inflammasome activation, thereby promoting atherosclerosis in systemic lupus erythematosus (SLE) [38]. Moreover, hepatocellular expression of CMPK2 drives the development of steatohepatitis by mediating metabolic dysfunction [39]. Furthermore, research has reported significant increased CMPK2 expression in pSS compared to healthy individuals, rendering it a promising biomarker for diagnosing pSS and assessing disease activity [38]. Cytochrome b-245 alpha chain (CYBA) encodes the p22/phox protein, which binds to NOX to form a complex that serves as a major source of cellular reactive oxygen species (ROS) [40]. In patients with OA, p22 is upregulated and regulates ROS production and IL-1β synthesis [41]. Additionally, by activating the NLRP3 inflammasome, P22 can induce N-GSDMD-dependent pyroptosis and the production of IL-1β and IL-18 [42]. In Aβ-induced retinal pigment epithelial cell injury, p22 activation triggers ROS production and mitochondrial dysfunction [43]. Collectively, these findings suggest that increased expression of IFI27, CMPK2, and CYBA in TED patients may accelerate the disease progression by exacerbating mitochondrial dysfunction and promoting ROS production and inflammation.

Metabolic status and immune processes engage in bidirectional crosstalk [44]. Immune dysregulation plays a critical role in the progression of TED. In this study, we use CIBERSORT to characterize the immune landscape in TED and identified higher enrichment of several immune cell populations, including follicular helper T (Tfh) cells, Monocytes, Macrophages M1 and Neutrophils in the TED group compared to the control group. Previous research has clearly demonstrated that TED patients exhibit higher neutrophil-to-lymphocyte ratio (NLR) and monocyte-to-HDL cholesterol ratio (MHR) than healthy controls, with elevated MHR and NLR values associated with more severe and active diseases [45]. $CD169^{+}$ classical monocytes accumulate in orbital tissue via the Cxcl12-Cxcr4 axis [46]. In active chronic inflammatory diseases, the number of $CD86^{+}$ M1-like macrophages increases significantly, which correlates closely with the activation of inflammatory activity [47]. Regulatory T (Treg) cells are essential for maintaining self-tolerance, and their elevation is linked to the pathogenesis of inflammatory diseases [48]. For instance, the dysregulated Treg cells in epithelial cells of obese patients can promote IL-17A-mediated psoriatic inflammation by enhancing IL-17A-driven inflammatory responses [49]. Additionally, the frequency of Treg cells is increased in patients with GO [50], where they interact with B cells to induce antibody production [51]. Mitochondrial metabolism exerts a substantial influence on the regulation of immune cell response. Studies have shown that mitochondrial dysfunction in macrophages inhibits the repolarization of M1 macrophages to M2 phenotype [52,53], mediates the immunoinflammatory microenvironment, and suppresses tissue repair after myocardial infarction [54]. The production of cellular reactive oxygen species (ROS) is primarily dependent on the mitochondrial respiratory chain, and impaired ROS production is beneficial for M2 macrophage polarization and anti-inflammatory responses [55]. Here, our correlation analysis revealed positive association between *Ifi27*, *Cmpk2*, *Cyba* and both Macrophages M1 and Neutrophils. Furthermore, *Ifi27* showed a negative correlation with naïve B cells, while *Cmpk2* was negatively associated with memory B cells. Researchers have confirmed that *Ifi27* exerts a pro-inflammatory effect by inducing the infiltration of pulmonary macrophages. Moreover, during the progression of liver cirrhosis, *Ifi27* induces the shift of macrophages toward an M1-like phenotype, thereby promoting the production of pro-inflammatory factors and oxidative stress [56]. High expression of *Cmpk2* in macrophages promotes neuroinflammation and brain damage following ischemic stroke [57]. Meanwhile, a study has confirmed that targeting *Cyba* can inhibit the inflammatory response of M1 macrophages by reducing the production of ROS, thereby alleviating acute liver injury [58]. Meanwhile, GSEA results indicate that high expression levels of IFI27 and CYBA are associated with type 1 diabetes, systemic lupus erythematosus, and asthma. All these diseases are linked to dysregulation of autoimmune cells. Therefore, mitochondrial metabolism may also regulate the progression of TED by mediating macrophage reprogramming.

Conclusion

In summary, bioinformatics analysis of TED uncovered previously unrecognized connections between the immunological microenvironment and mitochondrial

metabolism. Three potential prognostic biomarkers (*Ifi27*, *Cmpk2* and *Cyba*) associated with mitochondrial dysfunction were identified through machine learning, offering potential molecular targets for TED research and therapy. However, our study has certain limitations. First, we lacked experimental validation of the hub genes' roles (*Ifi27*, *Cmpk2* and *Cyba*) in inflammation and additional clinical data support. Secondly, despite the rigorous bioinformatics analyses conducted, the sample size of the original dataset used in the construction of the machine learning model in this study is relatively small, and further validation with a larger cohort is required in subsequent research. Furthermore, although GWAS results indicate that these genes are associated with the disease, additional follow-up experiments are still required for validation. Therefore, additional *in vivo* and *in vitro* studies, along with the collection of relevant clinical patient data, are still required to further validate the expression levels of these diagnostic biomarkers. This novel research direction will be the focus of our subsequent investigations.

Availability of Data and Materials

The datasets generated in this study are available in the GEO datasets (http://www.ncbi.nlm.nih.gov/geo/) and from the corresponding author on reasonable request.

Author Contributions

CJW: Manuscript writing and data analysis. KJ: Methodology and manuscript writing. JS, JYW and JXZ: Data analysis and interpretation. JY: Conception, design and supervision. All authors contributed to important editorial changes in the manuscript. All authors read and approved the final manuscript. All authors have participated sufficiently in the work and agreed to be accountable for all aspects of the work.

Ethics Approval and Consent to Participate

Not applicable.

Acknowledgment

Thanks to the National Center for Biotechnology Information (NCBI) Gene Expression Omnibus database and KEGG database for the great support.

Funding

This study was founded by the National Natural Science Foundation of China (Grant No. 82101178).

Conflict of Interest

The authors declare no conflict of interest.

Supplementary Material

Supplementary material associated with this article can be found, in the online version, at https://doi.org/10.24976/Discov.Med.202537200.166.

References

[1] Wiersinga WM, Eckstein AK, Žarković M. Thyroid eye disease (Graves' orbitopathy): clinical presentation, epidemiology, pathogenesis, and management. The Lancet. Diabetes & Endocrinology. 2025; 13: 600–614. https://doi.org/10.1016/S2213-8587(25)00066-X.

[2] Kiljanski J, Nebes V, Stachura I, Kennerdell JS, Wall JR. Should Graves' disease be considered a collagen disorder of the thyroid, skeletal muscle and connective tissue? Hormone and Metabolic Research = Hormon- Und Stoffwechselforschung = Hormones et Metabolisme. 1995; 27: 528–532. https://doi.org/10.1055/s-2007-980019.

[3] Bahn RS. Graves' ophthalmopathy. The New England Journal of Medicine. 2010; 362: 726–738. https://doi.org/10.1056/NEJMra0905750.

[4] Bartalena L, Baldeschi L, Boboridis K, Eckstein A, Kahaly GJ, Marcocci C, *et al*. The 2016 European Thyroid Association/European Group on Graves' Orbitopathy Guidelines for the Management of Graves' Orbitopathy. European Thyroid Journal. 2016; 5: 9–26. https://doi.org/10.1159/000443828.

[5] Bartalena L, Piantanida E, Gallo D, Lai A, Tanda ML. Epidemiology, Natural History, Risk Factors, and Prevention of Graves' Orbitopathy. Frontiers in Endocrinology. 2020; 11: 615993. https://doi.org/10.3389/fendo.2020.615993.

[6] Stan MN, Wagner LH, Rachmasari KN, Venker B, Arackal J, Wang J, *et al*. Epidemiology and Management of Moderate to Severe Thyroid Eye Disease in the United States: Analysis of a Healthcare Claims Database. Clinical Endocrinology. 2025; 102: 482–489. https://doi.org/10.1111/cen.15183.

[7] Shiber S, Stiebel-Kalish H, Shimon I, Grossman A, Robenshtok E. Glucocorticoid regimens for prevention of Graves' ophthalmopathy progression following radioiodine treatment: systematic review and meta-analysis. Thyroid: Official Journal of the American Thyroid Association. 2014; 24: 1515–1523. https://doi.org/10.1089/thy.2014.0218.

[8] Stan MN, Salvi M. MANAGEMENT OF ENDOCRINE DISEASE: Rituximab therapy for Graves' orbitopathy - lessons from randomized control trials. European Journal of Endocrinology. 2017; 176: R101–R109. https://doi.org/10.1530/EJE-16-0552.

[9] Smith TJ, Kahaly GJ, Ezra DG, Fleming JC, Dailey RA, Tang RA, *et al*. Teprotumumab for Thyroid-Associated Ophthalmopathy. The New England Journal of Medicine. 2017; 376: 1748–1761. https://doi.org/10.1056/NEJMoa1614949.

[10] Bartalena L, Kahaly GJ, Baldeschi L, Dayan CM, Eckstein A, Marcocci C, *et al*. The 2021 European Group on Graves' orbitopathy (EUGOGO) clinical practice guidelines for the medical management of Graves' orbitopathy. European Journal of Endocrinology. 2021; 185: G43–G67. https://doi.org/10.1530/EJE-21-0479.

[11] Glancy B. Visualizing Mitochondrial Form and Function within the Cell. Trends in Molecular Medicine. 2020; 26: 58–70. https://doi.org/10.1016/j.molmed.2019.09.009.

[12] Li Y, Chen H, Xie X, Yang B, Wang X, Zhang J, *et al*. PINK1-Mediated Mitophagy Promotes Oxidative Phosphorylation and Redox Homeostasis to Induce Drug-Tolerant Persister Cancer Cells. Cancer Research. 2023; 83: 398–413. https://doi.org/10.1158/0008-5472.CAN-22-2370.

[13] Huang Y, Zhou J, Wang S, Xiong J, Chen Y, Liu Y, *et al*. Indoxyl sulfate induces intestinal barrier injury through IRF1-DRP1 axis-mediated mitophagy impairment. Theranostics. 2020; 10: 7384–7400. https://doi.org/10.7150/thno.45455.

[14] Terluk MR, Kapphahn RJ, Soukup LM, Gong H, Gallardo C, Montezuma SR, *et al*. Investigating mitochondria as a target for treating age-related macular degeneration. The Journal of Neuroscience: the Official Journal of the Society for Neuroscience. 2015; 35: 7304–7311. https://doi.org/10.1523/JNEUROSCI.0190-15.2015.

[15] Missiroli S, Genovese I, Perrone M, Vezzani B, Vitto VAM, Giorgi C. The Role of Mitochondria in Inflammation: From Cancer to Neurodegenerative Disorders. Journal of Clinical Medicine. 2020; 9: 740. https://doi.org/10.3390/jcm9030740.

[16] Cai WW, Yu Y, Zong SY, Wei F. Metabolic reprogramming as a key regulator in the pathogenesis of rheumatoid arthritis. Inflammation Research: Official Journal of the European Histamine Research Society ... [et Al.]. 2020; 69: 1087–1101. https://doi.org/10.1007/s00011-020-01391-5.

[17] Buang N, Tapeng L, Gray V, Sardini A, Whilding C, Lightstone L, *et al*. Type I interferons affect the metabolic fitness of CD8$^+$ T cells from patients with systemic lupus erythematosus. Nature Communications. 2021; 12: 1980. https://doi.org/10.1038/s41467-021-22312-y.

[18] Zhang C, Ma Z, Nan X, Wang W, Zeng X, Chen J, *et al*. Comprehensive analysis to identify the influences of SARS-CoV-2 infections to inflammatory bowel disease. Frontiers in Immunology. 2023; 14: 1024041. https://doi.org/10.3389/fimmu.2023.1024041.

[19] Yu G, Wang LG, Han Y, He QY. clusterProfiler: an R package for comparing biological themes among gene clusters. Omics: a Journal of Integrative Biology. 2012; 16: 284–287. https://doi.org/10.1089/omi.2011.0118.

[20] Yin H, Lin M, Liang S, Wei M, Huang C, Qin F, *et al*. Ferroptosis-related gene signature predicts prognosis in kidney renal papillary cell carcinoma. Frontiers in Oncology. 2022; 12: 988867. https://doi.org/10.3389/fonc.2022.988867.

[21] Ritchie ME, Phipson B, Wu D, Hu Y, Law CW, Shi W, *et al*. limma powers differential expression analyses for RNA-sequencing and microarray studies. Nucleic Acids Research. 2015; 43: e47. https://doi.org/10.1093/nar/gkv007.

[22] Chen Y, Li ZY, Zhou GQ, Sun Y. An Immune-Related Gene Prognostic Index for Head and Neck Squamous Cell Carcinoma. Clinical Cancer Research: an Official Journal of the American Association for Cancer Research. 2021; 27: 330–341. https://doi.org/10.1158/1078-0432.CCR-20-2166.

[23] Gustavsson EK, Zhang D, Reynolds RH, Garcia-Ruiz S, Ryten M. ggtranscript: an R package for the visualization and interpretation of transcript isoforms using ggplot2. Bioinformatics (Oxford, England). 2022; 38: 3844–3846. https://doi.org/10.1093/bioinformatics/btac409.

[24] Gu Z, Eils R, Schlesner M. Complex heatmaps reveal patterns and correlations in multidimensional genomic data. Bioinformatics (Oxford, England). 2016; 32: 2847–2849. https://doi.org/10.1093/bioinformatics/btw313.

[25] Bardou P, Mariette J, Escudié F, Djemiel C, Klopp C. jvenn: an interactive Venn diagram viewer. BMC Bioinformatics. 2014; 15: 293. https://doi.org/10.1186/1471-2105-15-293.

[26] Davis AP, Grondin CJ, Johnson RJ, Sciaky D, McMorran R, Wiegers J, *et al*. The Comparative Toxicogenomics Database: update 2019. Nucleic Acids Research. 2019; 47: D948–D954. https://doi.org/10.1093/nar/gky868.

[27] Zhou G, Soufan O, Ewald J, Hancock REW, Basu N, Xia J. NetworkAnalyst 3.0: a visual analytics platform for comprehensive gene expression profiling and meta-analysis. Nucleic Acids Research. 2019; 47: W234–W241. https://doi.org/10.1093/nar/gkz240.

[28] Subramanian A, Tamayo P, Mootha VK, Mukherjee S, Ebert BL, Gillette MA, *et al*. Gene set enrichment analysis: a knowledge-based approach for interpreting genome-wide expression profiles. Proceedings of the National Academy of Sciences of the United States of America. 2005; 102: 15545–15550. https://doi.org/10.1073/pnas.0506580102.

[29] Zhu J, Lu Q, Liang T, JieJiang, Li H, Zhou C, *et al*. Development and Validation of a Machine Learning-Based Nomogram for Prediction of Ankylosing Spondylitis. Rheumatology and Therapy. 2022; 9: 1377–1397. https://doi.org/10.1007/s40744-022-00481-6.

[30] Tian L, Wu W, Yu T. Graph Random Forest: A Graph Embedded Algorithm for Identifying Highly Connected Important Features. Biomolecules. 2023; 13: 1153. https://doi.org/10.3390/biom13071153.

[31] Nie T, Lamb YN. Teprotumumab: A Review in Thyroid Eye Disease. Drugs. 2022; 82: 1663–1670. https://doi.org/10.1007/s40265-022-01804-1.

[32] Taylor PN, Zhang L, Lee RWJ, Muller I, Ezra DG, Dayan CM, *et al*. New insights into the pathogenesis and nonsurgical management of Graves orbitopathy. Nature Reviews. Endocrinology. 2020; 16: 104–116. https://doi.org/10.1038/s41574-019-0305-4.

[33] VanPortfliet JJ, Lei Y, Ramanathan M, Martinez CG, Wong J, Stodola TJ, *et al*. Caspase-11 drives macrophage hyperinflammation in models of Polg-related mitochondrial disease. Nature Communications. 2025; 16: 4640. https://doi.org/10.1038/s41467-025-59907-8.

[34] Kimoto O, Sawada J, Shimoyama K, Suzuki D, Nakamura S, Hayashi H, *et al*. Activation of the interferon pathway in peripheral blood of patients with Sjogren's syndrome. The Journal of Rheumatology. 2011; 38: 310–316. https://doi.org/10.3899/jrheum.100486.

[35] Zhang Y, Chen C, Liu Z, Guo H, Lu W, Hu W, *et al*. PABPC1-induced stabilization of IFI27 mRNA promotes angiogenesis and malignant progression in esophageal squamous cell carcinoma through exosomal miRNA-21-5p. Journal of Experimental & Clinical Cancer Research: CR. 2022; 41: 111. https://doi.org/10.1186/s13046-022-02339-9.

[36] Arumugam P, Singla M, Lodha R, Rao V. Identification and characterization of novel infection associated transcripts in macrophages. RNA Biology. 2021; 18: 604–611. https://doi.org/10.1080/15476286.2021.1989217.

[37] Zhao M, Su HZ, Zeng YH, Sun Y, Guo XX, Li YL, *et al*. Loss of function of CMPK2 causes mitochondria deficiency and brain calcification. Cell Discovery. 2022; 8: 128. https://doi.org/10.1038/s41421-022-00475-2.

[38] Li N, Li Y, Hu J, Wu Y, Yang J, Fan H, *et al*. A Link Between Mitochondrial Dysfunction and the Immune Microenvironment of Salivary Glands in Primary Sjogren's Syndrome. Frontiers in Immunology. 2022; 13: 845209. https://doi.org/10.3389/fimmu.2022.845209.

[39] Zhu S, Liao L, Zhong Y, Liu Z, Lu J, Yang Z, *et al*. Hepatocellular CMPK2 promotes the development of metabolic dysfunction-associated steatohepatitis. Journal of Hepatology. 2025; 83: 383–396. https://doi.org/10.1016/j.jhep.2025.01.008.

[40] Stasia MJ. CYBA encoding p22(phox), the cytochrome b558 alpha polypeptide: gene structure, expression, role and physiopathology. Gene. 2016; 586: 27–35. https://doi.org/10.1016/j.gene.2016.03.050.

[41] Niu H, Deng X, Zhang Q, Zhao Y, Wen J, Li W, *et al*. Identification and Verification of Hub Mitochondrial Dysfunction Genes in Osteoarthritis Based on Bioinformatics Analysis. Journal of Immunology Research. 2024; 2024: 6822664. https://doi.org/10.1155/2024/6822664.

[42] Chen N, Chen P, Zhou Y, Chen S, Gong S, Fu M, *et al*. HuNoV Non-Structural Protein P22 Induces Maturation of IL-1β and IL-18 and N-GSDMD-Dependent Pyroptosis through Activating NLRP3 Inflammasome. Vaccines. 2023; 11: 993. https://doi.org/10.3390/vaccines11050993.

[43] Sun J, Chen J, Li T, Huang P, Li J, Shen M, *et al*. ROS production and mitochondrial dysfunction driven by PU.1-regulated NOX4-p22^{phox} activation in Aβ-induced retinal pigment epithelial cell injury. Theranostics. 2020; 10: 11637–11655. https://doi.org/10.7150/thno.48064.

[44] Makowski L, Chaib M, Rathmell JC. Immunometabolism: From basic mechanisms to translation. Immunological Reviews. 2020; 295: 5–14. https://doi.org/10.1111/imr.12858.

[45] Yılmaz Tuğan B, Ergen A, Özkan B. Monocyte-to-high-density lipoprotein ratio and systemic immune-inflammation index: Potential parameters for the evaluation of disease activity and severity in Graves' ophthalmopathy? International Ophthalmology. 2024; 44: 154. https://doi.org/10.1007/s10792-024-03077-x.

[46] Wang D, Ling J, Tan R, Wang H, Qu Y, Li X, *et al*. CD169^{+} classical monocyte as an important participant in Graves' ophthalmopathy through CXCL12-CXCR4 axis. iScience. 2024; 27: 109213. https://doi.org/10.1016/j.isci.2024.109213.

[47] Lu Y, Wang Y, Wang Y, Wu Y, Huang Y, Liu X, *et al*. M1-Like Macrophages Modulate Fibrosis and Inflammation of Orbital Fibroblasts in Graves' Orbitopathy: Potential Relevance to Soluble Interleukin-6 Receptor. Thyroid: Official Journal of the American Thyroid Association. 2023; 33: 338–350. https://doi.org/10.1089/thy.2022.0254.

[48] Zhang J, Ren M, Zeng H, Guo Y, Zhuang Z, Feng Z, *et al*. Elevated follicular helper T cells and expression of IL-21 in thyroid tissues are involved in the pathogenesis of Graves' disease. Immunologic Research. 2015; 62: 163–174. https://doi.org/10.1007/s12026-015-8647-z.

[49] Sivasami P, Elkins C, Diaz-Saldana PP, Goss K, Peng A, Hamersky M, 4th, *et al*. Obesity-induced dysregulation of skin-resident PPARγ^{+} Treg cells promotes IL-17A-mediated psoriatic inflammation. Immunity. 2023; 56: 1844–1861.e6. https://doi.org/10.1016/j.immuni.2023.06.021.

[50] Zhu C, Ma J, Liu Y, Tong J, Tian J, Chen J, *et al*. Increased frequency of follicular helper T cells in patients with autoimmune thyroid disease. The Journal of Clinical Endocrinology and Metabolism. 2012; 97: 943–950. https://doi.org/10.1210/jc.2011-2003.

[51] Gensous N, Charrier M, Duluc D, Contin-Bordes C, Truchetet ME, Lazaro E, *et al*. T Follicular Helper Cells in Autoimmune Disorders. Frontiers in Immunology. 2018; 9: 1637. https://doi.org/10.3389/fimmu.2018.01637.

[52] Cai S, Zhao M, Zhou B, Yoshii A, Bugg D, Villet O, *et al*. Mitochondrial dysfunction in macrophages promotes inflammation and suppresses repair after myocardial infarction. The Journal of Clinical Investigation. 2023; 133: e159498. https://doi.org/10.1172/JCI159498.

[53] Van den Bossche J, Baardman J, Otto NA, van der Velden S, Neele AE, van den Berg SM, *et al*. Mitochondrial Dysfunction Prevents Repolarization of Inflammatory Macrophages. Cell Reports. 2016; 17: 684–696. https://doi.org/10.1016/j.celrep.2016.09.008.

[54] Dong T, Chen X, Xu H, Song Y, Wang H, Gao Y, *et al*. Mitochondrial metabolism mediated macrophage polarization in chronic lung diseases. Pharmacology & Therapeutics. 2022; 239: 108208. https://doi.org/10.1016/j.pharmthera.2022.108208.

[55] Tantawy MA, Hatesuer B, Wilk E, Dengler L, Kasnitz N, Weiß S, *et al*. The interferon-induced gene Ifi27l2a is active in lung macrophages and lymphocytes after influenza A infection but deletion of Ifi27l2a in mice does not increase susceptibility to infection. PloS One. 2014; 9: e106392. https://doi.org/10.1371/journal.pone.0106392.

[56] Xiong Z, Chen P, Yuan M, Yao L, Wang Z, Liu P, *et al*. Integrated Bioinformatics and Validation Reveal *IFI27* and Its Related Molecules as Potential Identifying Genes in Liver Cirrhosis. Biomolecules. 2023; 14: 13. https://doi.org/10.3390/biom14010013.

[57] Guan X, Zhu S, Song J, Liu K, Liu M, Xie L, *et al*. Microglial CMPK2 promotes neuroinflammation and brain injury after ischemic stroke. Cell Reports. Medicine. 2024; 5: 101522. https://doi.org/10.1016/j.xcrm.2024.101522.

[58] Li H, Chen J, Guo H, Yang H, Liu J, Yuan H, *et al*. Integrated transcriptomic and proteomic profiling reveals the anti-inflammatory mechanism of dihydroartemisinin in the treatment of acute liver injury by targeting CYBA and CYBB. Biochemical and Biophysical Research Communications. 2025; 764: 151821. https://doi.org/10.1016/j.bbrc.2025.151821.